



Kahramanmaraş Sutcu Imam University

Journal of Engineering Sciences



Geliş Tarihi : 06.09.2023
Kabul Tarihi : 13.10.2023

Received Date : 06.09.2023
Accepted Date : 13.10.2023

BLOOD PRESSURE AND HEART RATE ESTIMATION VIA TQWT BASED DECOMPOSITION OF PPG SIGNALS

PPG SİNYALLERİNİN TQWT TABANLI AYRIŞTIRILMASI YOLUYLA KAN BASINCI VE KALP ATIŞ HIZI TAHMİNİ

*Fatma Sevde KÖKLÜKAYA*¹ (ORCID: 0000-0002-9348-0925)
Mahmut ÖZTÜRK^{1*} (ORCID: 0000-0003-2600-7051)

¹ Istanbul University - Cerrahpaşa, Department of Electrical and Electronics Engineering, Istanbul, Türkiye

*Sorumlu Yazar / Corresponding Author: Mahmut ÖZTÜRK, mahmutoz@iuc.edu.tr

ABSTRACT

Photoplethysmography (PPG) signals are getting more popular and promising for medical applications because of the non-invasive, fast, and simple recording techniques. Using PPG signals for monitoring the blood pressure (BP) and heart rate (HR) levels instead of traditional invasive and cuff-based measurement techniques is possible and continuous tracing of BP and HR levels can be accomplished with high measurement accuracies. These developments are very important and helpful, especially for people suffering from high tension and cardiac problems. In this study, we propose to use Tunable Q-factor Wavelet Transform (TQWT) for decomposing the PPG signals into sub-signals and extracting some statistical features from each of the sub-signals and main signal. Artificial Neural Networks (ANN), Random Forests (RF), and Support Vector Machines (SVM) algorithms are employed to estimate diastolic blood pressure (DBP), systolic blood pressure (SBP), and heart rate (HR) values. PPG signals, DBP, SBP, and HR values which were measured with traditional methods were obtained from the open dataset of Guilin People's Hospital of China. This dataset includes information of 219 individuals. Each machine learning method was applied to the features separately, and the results of the regression analysis were interpreted by using the error rates and correlations between the actual and estimated values. Results show that the RF algorithm is more successful than ANN and SVM for the estimation of DBP, SBP, and HR levels.

Keywords: Photoplethysmography, TQWT, machine learning, blood pressure, heart rate

ÖZET

Fotoplethysmografi (PPG) sinyalleri, invaziv olmayan, hızlı ve basit kayıt teknikleri nedeniyle tıbbi uygulamalar için daha popüler ve umut verici hale geliyor. Kan basıncını (KB) ve kalp atış hızı (KAH) seviyelerini izlemek için geleneksel invaziv ve manşet tabanlı ölçüm teknikleri yerine PPG sinyallerinin kullanılması mümkündür ve KB ve KAH seviyelerinin sürekli takibi, yüksek ölçüm doğruluklarıyla gerçekleştirilebilir. Bu gelişmeler özellikle yüksek tansiyon ve kalp sorunu yaşayan kişiler için çok önemli ve faydalıdır. Bu çalışmada, PPG sinyallerini alt sinyallere ayırtmak ve her bir alt sinyalden ve ana sinyalden bazı istatistiksel özellikler çıkarmak için Ayarlanabilir Q-faktörü Dalgacık Dönüşümü'nü (TQWT) kullanmayı öneriyoruz. Diastolik kan basıncı (DKB), sistolik kan basıncı (SKB) ve kalp atış hızı (KAH) değerlerinin tahmin edilmesinde Yapay Sinir Ağları (YSA), Rastgele Ormanlar (RF) ve Destek Vektör Makineleri (SVM) algoritmaları kullanılmaktadır. Geleneksel yöntemlerle ölçülen PPG sinyalleri, DKB, SKB ve KAH değerleri Çin Guilin Halk Hastanesi'nin açık veri setinden elde edildi. Bu veri seti 219 kişinin bilgilerini içermektedir. Her bir makine öğrenmesi yöntemi, özelliklere ayrı ayrı uygulanmış ve regresyon analizi sonuçları, hata oranları ve gerçek ve tahmin edilen değerler arasındaki korelasyonlar kullanılarak yorumlanmıştır. Sonuçlar RF algoritmasının DKB, SKB ve KAH seviyelerinin tahmininde YSA ve SVM'den daha başarılı olduğunu göstermektedir.

Anahtar Kelimeler: Fotoplethysmografi, TQWT, makine öğrenimi, kan basıncı, kalp atış hızı

ToCite: KÖKLÜKAYA, F. S., & ÖZTÜRK, M., (2023). BLOOD PRESSURE AND HEART RATE ESTIMATION VIA TQWT BASED DECOMPOSITION OF PPG SIGNALS. *Kahramanmaraş Sütçü İmam Üniversitesi Mühendislik Bilimleri Dergisi*. 26(4), 1050-1060.

INTRODUCTION

Today, with the advancements in biomedical device technologies, the measurements needed for the diagnosis and monitoring of patient's health problems can be performed non-invasively and conveniently, without causing patient discomfort and requiring surgical procedures. The optical measurement method called photoplethysmography used for measurements such as heart rate and blood pressure (BP) is among the most commonly used methods today (Kraitl and Hartmut, 2005). Hertzman introduced the PPG technique for the first time in 1937 (Hertzman, 1938).

Photoplethysmography (PPG) signals are frequently used especially in the research and investigation of vascular diseases thanks to the ease of use and cost-effectiveness of the method. In scientific studies conducted with the PPG signals, some important physiological parameters such as BP, respiratory data, and heart rate (HR) have been extracted from these signals and used as an alternative to biological signals (Nafisi and Shahabi, 2018; Bagha and Shaw, 2011; Allen, 2007). In the first years of the PPG method had been introduced, it was used to determine a limited number of physiological characteristics such as HR and heart rate variations (HRV). However, thanks to the studies that continue today, it has been determined that PPG signals contain many physiological parameters of the individuals (Übeyli et al., 2010). There is a plethora of studies in the literature using many characteristics extracted from the PPG signals. Some of the characteristics investigated are the number of PPG pulses, signal amplification time, pulse transit time (PTT), pulse arrival time (PAT), amplitude, normalized PPG pulse shape, pulse width, and pulse height (Allen and Murray, 2003).

The PPG signals have been the subject of a vast number of studies in the last decades. The most common and fundamental one among these studies is the detection of pulse rate using the PPG signals. Shin H. S. et al. have developed the adaptive threshold method and detected the peak points of the PPG signals (Shin et al., 2009). The PPG signals have two peak points: systolic and diastolic (Mc Duff et al., 2014). The systolic peak shows the moment the heart pumps blood to the body, and the diastolic peak shows the moment of closure of the aortic valves (Yousef et al., 2012). In their study, Shin H. S. et al. (Shin et al., 2009) determined the adaptive threshold value and the systolic peaks of the PPG. In the study presented by Johnston, methods estimating arterial saturation, HR, HRV, and respiratory rate based on the PPG signals have been investigated (Johnston, 2006).

It is possible to measure the BP using invasive or non-invasive methods. Invasive measurement is definitely more accurate, but it is applicable only in clinics or hospitals. The most common non-invasive BP measurement technique is the use of the traditional cuff sphygmomanometer. Only experienced people can use this device and it is not comfortable and useful in daily routines of patients. Using the PPG signals to monitor BP has become more popular and easier in the last decades. It is a non-invasive and cuffless measurement technique. This makes it possible to use it often in daily life and monitor the BP level. A smartwatch or even a simple wrist can be used to sense PPG signals and estimate the BP levels using these signals.

In the last decade, many researches have been done to estimate BP using PPG signals. Kurylyak et al. obtained time-domain features from PPG waveforms and estimated systolic blood pressure (SBP) and diastolic blood pressure (DBP) using an Artificial Neural Network (ANN) (Kurylyak et al., 2013). Teng and Zhang presented a linear regression model to estimate BP using the PPG signals (Teng and Zhang, 2003). Their results achieved the standards of the American National Standards of the Association for the Advancement of Medical Instrumentation (AAMI) (ANSI, 2017). Xing and Sun proposed to use of frequency domain features of PPG signals and a feedforward neural network for estimating the BP levels (Xing and Sun, 2016). They obtained power spectrums of PPG signals first and obtained features from amplitudes and shapes of the power spectrums. Gao et al. proposed a new BP estimation approach using discrete wavelet transform (DWT) and support vector machine (SVM) (Gao et al., 2016).

Some researchers preferred to use time domain and frequency domain features together. Using time-frequency analysis methods at feature extraction stage is the most convenient approach in these researches. Rastegar et al. used continuous wavelet transform (CWT) to obtain scalograms of PPG and ECG signals (Rastegar et al., 2019). Then, they fed a convolutional neural network (CNN) with the images of scalograms to estimate the BP. In the method presented by Schlesinger et al., spectrograms of the PPG signals were obtained, and spectro-temporal features were extracted using them (Schlesinger et al., 2020). Encouraging results were reported for TF based approaches.

METHODOLOGY

In this study, we propose a decomposition based approach to estimate the SBP, the DBP, and HRV from PPG signals using machine learning methods. The PPG signals were decomposed into their sub-bands using the Tunable Q-Factor Wavelet Transform (TQWT) (Selesnick, 2011) method, and the features were extracted from each sub-band separately. The TQWT was preferred because of its high representation capability for random signals like PPG. Width and fluctuations of the mother wavelet can be changed easily and effectively with the TQWT method. Thus, the mother wavelet can be arranged depending on the time-varying frequency of random signals. For estimating the BP and HR values, artificial neural networks (ANN), random forests (RF), and support vector machines (SVM) were employed as the machine learning methods. These methods were employed in regression analysis mode using the Weka software.

We obtained the PPG signals from the open dataset shared by Guilin People's Hospital, China (Liang et al., 2018). The dataset includes PPG records of 219 individuals with SBP, DBP, and HRV levels. The individuals aged between 21 and 86. 104 of them are males and 115 are females. Duration of each PPG segment is 2,1 seconds and the dataset contains 3 different PPG segments for each individual. Sampling frequency is 1 kHz.

PPG Acquisition, Blood Pressure and Heart Rate Levels

PPG signals can be measured in areas where there are many capillary vessels such as fingertips and earlobes as well as the wrists. During this measurement, an LED emitting light at a certain wavelength as a transmitter, and a photodiode sensitive to such wavelength, which also functions as a receiver, are used in the sensor part. PPG can also be measured on protrusions such as fingertips, toes, forehead, and earlobes (Allen, 2007; Allen and Murray, 2003). As PPG signals are measured on areas outside the trunk, especially on the fingers or ears, they are easier to acquire and process, painless, and more practical compared with conventional medical methods.

Table 1. Classification of BP Levels for Adults (Büyüköztürk, 1999)

Tension Classes	SBP		DBP
Optimal	< 120	and	< 80
Normal	< 130	and	< 85
High-Normal	130-139	or	85-89
Hypertension			
Stage 1	140-159	or	90-99
Stage 2	160-179	or	100-109
Stage 3	≥180	or	≥110
Isolated Systolic Hypertension	140-160	and	< 90
Isolated Systolic Hypertension (at the border)	≥160	and	< 90

Hypertension refers to an increase in arterial blood pressure (ABP) above normal values. Today, an SBP ≥ 140 mmHg and a DBP ≥ 90 mmHg or the individual needing to use antihypertensive medication is defined as hypertension (Büyüköztürk, 1999). In adults, BP levels are classified qualitatively. However, in practice, it is important for doctors to take BP values into consideration for convenience of diagnosis and treatment. BPs of adults at the age of 18 or above are divided into four groups, which are optimal, normal, high-normal, and hypertension. As can be seen in Table 1, optimal BP values are lower than 120/80 mmHg. Normal BP is indicated to be lower than 130/85 mmHg. If BP values are 130-139/85-89 mmHg, it is classified as high-normal tension. The values higher than 140/90 are considered as hypertension (Büyüköztürk, 1999).

The biological data called the heart rate or the pulse contains important information about the physiological state of the human body. For example, resting pulse value is a primary indicator in the detection of heart diseases (Liang et al., 2018). In the last decade, heart rate and pulse measurement with PPG have become popular as an alternative to recording heart beat signals with the conventional electrocardiogram (ECG), which has a history of approximately 100 years.

Tunable Q-Factor Wavelet Transform (TQWT)

Analysis of random signals such as PPG is challenging because of their oscillatory and unpredictable nature. As the TQWT is adjusted according to the oscillations, it is a successful method in the analysis of such signals. The TQWT, developed by Selesnick (Selesnick, 2011), is a signal analysis technique that has the capability of easily determining the Q-factor. Thereby, the technique allows to adjust the wavelet transformation according to the signal's oscillation.

Q-factor is the ratio of the central frequency of an oscillating signal to its bandwidth. In this method, as the frequency of the analyzed signal increases, the Q-factor is adaptively increased. An increase in the Q-factor practically means an increase in the number of oscillations of the wavelet. Depending on the variations in the frequency of the signal, the number of oscillations of the mother wavelet is increased or decreased. Thus, a quite successful wavelet transformation is achieved for the analysis of especially non-stationary signals. Thanks to these characteristics, TQWT has become one of the most successful models employed for wavelet transformation. As the biomedical signals also have the non-stationary and oscillatory nature, their transformation using the TQWT method for both the time-frequency analysis and decomposition of the signal into sub-bands yields successful results. The TQWT method is promising for the studies conducted with biomedical signals.

The decomposition process using TQWT can be controlled by changing three tunable parameters. These are Q-factor (Q), redundancy (r), and the number of decomposition levels (J). Each decomposition is performed using low-pass and high-pass filters in this method. If the sampling frequency of the main signal $s[n]$ is f_s , low-pass and high-pass sub-band signals are expressed with the sampling frequencies αf_s and βf_s respectively. Frequency responses of the low-pass, $H_0^J(\omega)$, and the high-pass, $H_1^J(\omega)$, filters are shown as (Selesnick, 2011):

$$H_0^J(\omega) = \begin{cases} \prod_{m=0}^{J-1} H_0(\omega/\alpha^m), & |\omega| \leq \alpha^J \pi \\ 0, & \alpha^J \pi < |\omega| \leq \pi \end{cases} \quad (1)$$

$$H_1^J(\omega) = \begin{cases} H_1(\omega/\alpha^{J-1}) \prod_{m=0}^{J-2} H_0(\omega/\alpha^m), & (1-\beta)\alpha^{J-1}\pi \leq |\omega| \leq \alpha^{J-1}\pi \\ 0, & \text{for other } \omega \in [-\pi, \pi], \end{cases} \quad (2)$$

where,

$$H_0(\omega) = \theta\left(\frac{\omega+(\beta-1)\pi}{\alpha+\beta-1}\right) \quad (3)$$

$$H_1(\omega) = \theta\left(\frac{\alpha\pi-\omega}{\alpha+\beta-1}\right) \quad (4)$$

$\theta(\omega)$ can be expressed as:

$$\theta(\omega) = 0.5(1 + \cos\omega)\sqrt{2 - \cos\omega}, \quad |\omega| \leq \pi \quad (5)$$

and it is the frequency response of the Daubechies filter. The parameters α and β that changes the scaling of signal spectrum can be arranged by r and Q as below (Selesnick, 2011):

$$r = \frac{\beta}{1-\alpha}, \quad Q = \frac{2-\beta}{\beta}. \quad (6)$$

Feature Extraction and Machine Learning

The choice of the features is very important for the success of regression analysis. Features must be selective as much as possible. In this study, we preferred to use most common time-domain features and the entropy features as a first step. More features can be tried and other domains should be used for feature extraction for obtaining better estimation results. We calculated and saved the absolute mean value, standard deviation, skewness, kurtosis and average power of each sub-signal and the main signal. Also, we calculated and saved the ratio of the absolute mean values of each adjacent sub-signals. Then, we calculated entropy features and saved them with other features. The calculated entropy features are shannon entropy, log-energy entropy, and normalized entropy (Acharya et al., 2018).

The chosen features are calculated as below (Ghayab et al., 2019; Acharya et al., 2018):

$$\text{Absolute Mean:} \quad X_{AbsMean} = \left| \frac{1}{N} \sum_{i=1}^N x_i \right| \quad (7)$$

$$\text{Standard Deviation:} \quad X_{Std} = \sqrt{\sum_{i=1}^N (x_i - X_{mean})^2 / (N-1)} \quad (8)$$

$$\text{Skewness:} \quad X_{Ske} = \sum_{i=1}^N (x_i - X_{mean}) \frac{3}{(N-1)X_{Std}^3} \quad (9)$$

$$\text{Kurtosis:} \quad X_{ku} = \frac{\sum_{i=1}^N (x_i - X_{mean})^4}{(N-1)X_{std}^4} \quad (10)$$

$$\text{Average Power:} \quad X_{power} = \frac{1}{N} \sum_{i=1}^N x_i^2 \quad (11)$$

$$\text{Shannon Entropy:} \quad E_{Shan} = -\sum_{n=1}^x P(S_n) \log_2(P(S_n)) \quad (12)$$

$$\text{Log-Energy Entropy:} \quad E_{Log-En} = \sum_{n=1}^x \log(S_n^2) \quad (13)$$

$$\text{Normalized Entropy:} \quad E_{Norm} = \sum_n |S_n|^k, \quad \text{with } 1 \leq k \quad (14)$$

In this study, machine learning methods were performed using the Weka open source software. This software contains regression, classification and clustering algorithms in addition to preprocessing methods (Engel et al., 2014). Regression analysis was applied to the matrices of the features obtained from PPG sub-band signals by using ANN, RF, and SVM algorithms in the Weka software. At the results of the analysis, SBP, DBP and HR levels were estimated with each of the machine learning methods separately. The machine learning methods used for regression analysis are summarized as follows.

Artificial Neural Networks (ANN)

ANNs are formed as a linked group of neurons. Neurons are grouped as input, output and hidden layers. All neurons are connected with the neurons of neighbor layers. Connections are done with the weighted links. By changing the values of the weights between neurons, output classes or values can be predicted for different inputs. The most common ANN architecture is the multilayer feed forward network. The main advantages of ANNs are the high classification capacity for patterns, robustness against the noisy input and fast computation ability because of the parallel network design (Han et al., 2011). In this work, we preferred to use multilayer feed forward network with backpropagation. We employed two hidden layers beside input and output layers. Input layer includes 143 neurons because of the number of features and the output layer includes 3 neurons because of the number of results.

Random Forests (RF)

RF is an ensemble of the decision tree classifiers. A basic decision tree selects the features randomly and forms random subsets at each node. Thus, it specifies the division. Every decision tree in the RF structure chooses a class. The mostly chosen one becomes the output RF algorithm (Han et al., 2011). In this work, we preferred to use classical RF algorithm.

Support Vector Machines (SVM)

SVM forms support vectors and margins to separate features using hyper-planes. Data can be distinguished depending on the position of it and the boundaries of the hyper-planes. The main advantage of SVM is the high accuracy obtaining capability in non-linear prediction cases. Also, they are very robust against the overfitting problem (Han et al., 2011). In this work, we used classical linear SVM algorithm.

EXPERIMENTS AND RESULTS

The TQWT parameters used in the experiments were as follows: Q=3, r=4, J=15. This means, each PPG signals were decomposed into 15 sub-bands. With the addition of the main signal, we have 16 sub-signals instead of main signal for feature extraction. A total of 143 features were calculated for each main PPG signal.

Approximately 2/3 of the data obtained from the dataset were used for training, and 1/3 for testing. The parameters of Correlation Coefficient (CC), Mean Absolute Error (MAE), and Root Mean Square Error (RMSE) were used for performance analysis. Mathematical expressions of these parameters can be seen below:

$$CC = \frac{N \sum xy - \sum x \sum y}{\sqrt{[N \sum x^2 - (\sum x)^2][N \sum y^2 - (\sum y)^2]}} \quad (12)$$

$$MAE = \frac{1}{m} \sum_{i=1}^m |x - y| \quad (13)$$

$$RMSE = \sqrt{\frac{1}{m} \sum_{i=1}^m |x - y|^2} \quad (14)$$

In the equations (12), (13), and (14), x and y show the estimated and reference values respectively. The correlation coefficients and error rates of the DBP, SBP and HR values estimated by analyzing the features obtained by the TQWT method using the algorithms of ANN, RF, and SVM are provided in Table 2, Table 3, and Table 4, respectively. The correlation coefficient in the estimations made using the RF algorithm is higher than the correlations coefficients in the estimations made using the ANN and SVM algorithms. Whereas the error rates in the estimations made using the RF and SVM algorithms are close to each other. However, the error rates in the estimations made using the ANN algorithm appear to be higher than the other algorithms.

The estimation performances of machine learning methods are shown in Tables 2, 3, and 4. Actual and predicted values of DBP, SBP and HR are shown in the figures below. DBP estimations performed using ANN, RF and SVM methods are shown in Figures 1, 2, and 3.

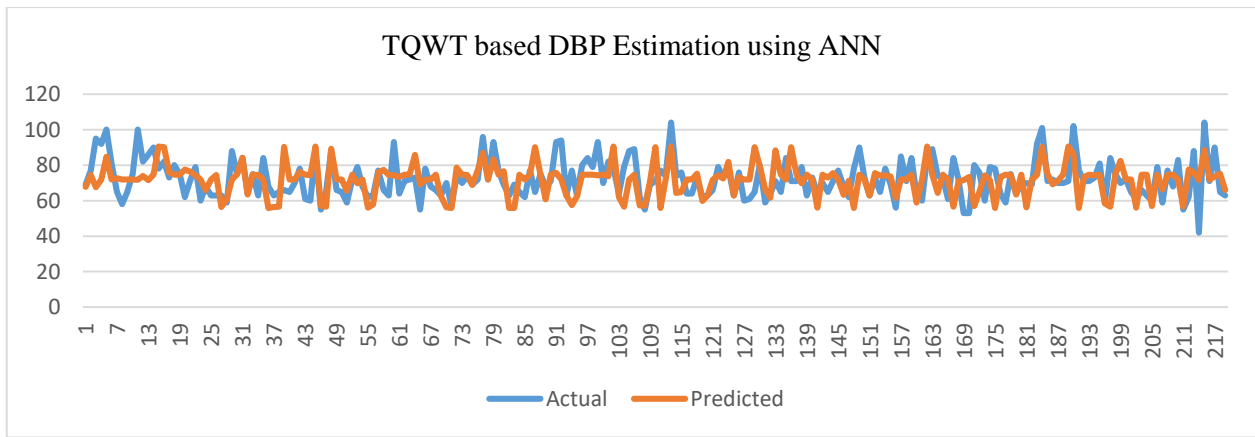


Figure 1. TQWT based DBP Estimation using ANN

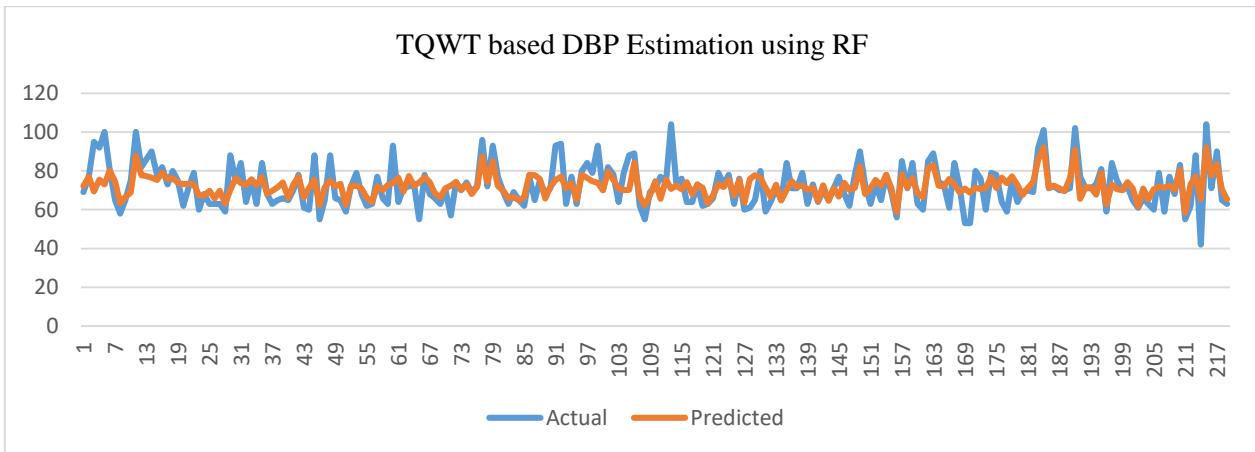


Figure 2. TQWT based DBP Estimation using RF

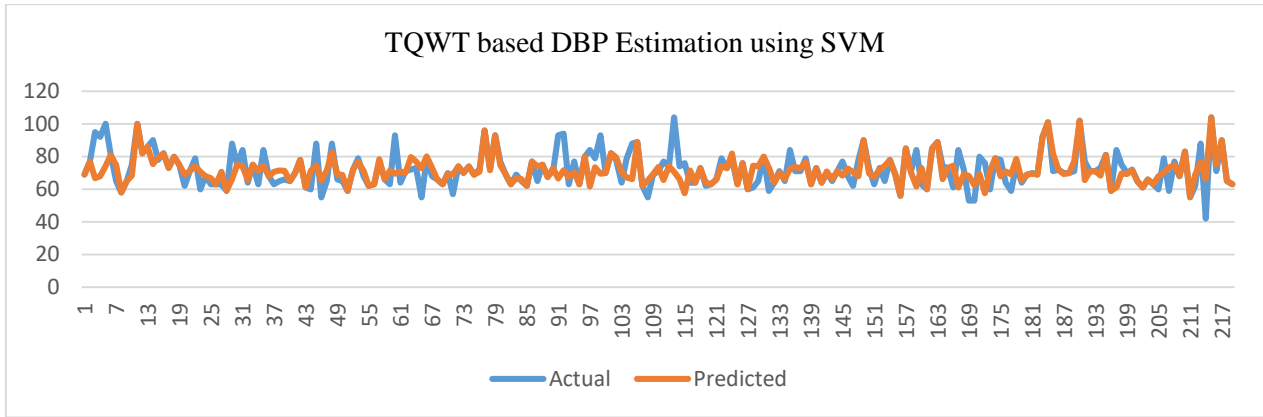


Figure 3. TQWT based DBP Estimation using SVM

Table 2. Normalized Correlations and Error Rates for TQWT based DBP Estimation

Method	CC	MAE (mmHg)	RMSE (mmHg)
ANN	0.4122	8.0119	9.1953
RF	0.7219	4.4732	6.9235
SVM	0.6714	3.8891	6.1135

SBP estimations performed using ANN, RF and SVM algorithms can be seen in Figures 4, 5, and 6.

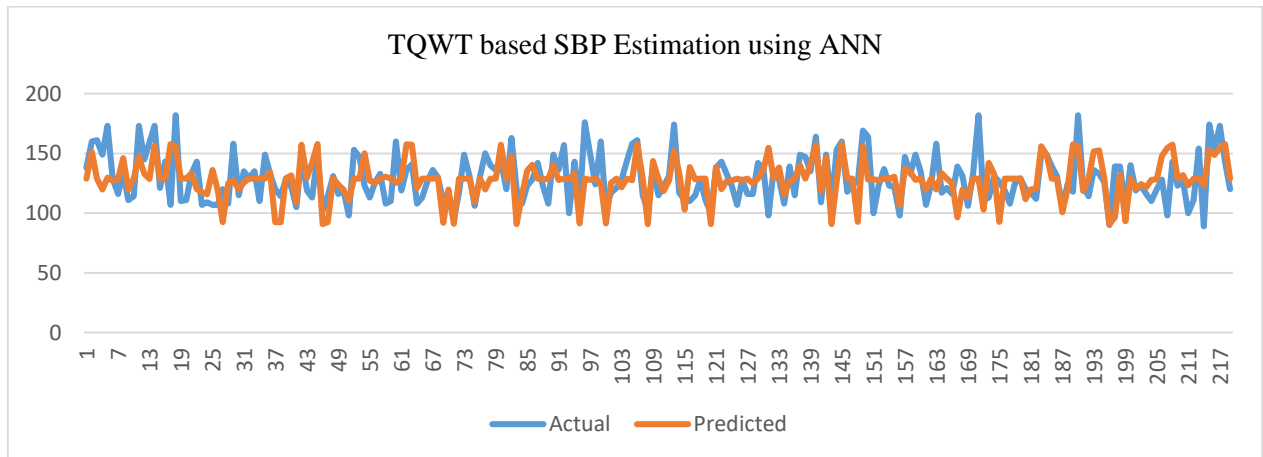


Figure 4. TQWT based SBP Estimation using ANN

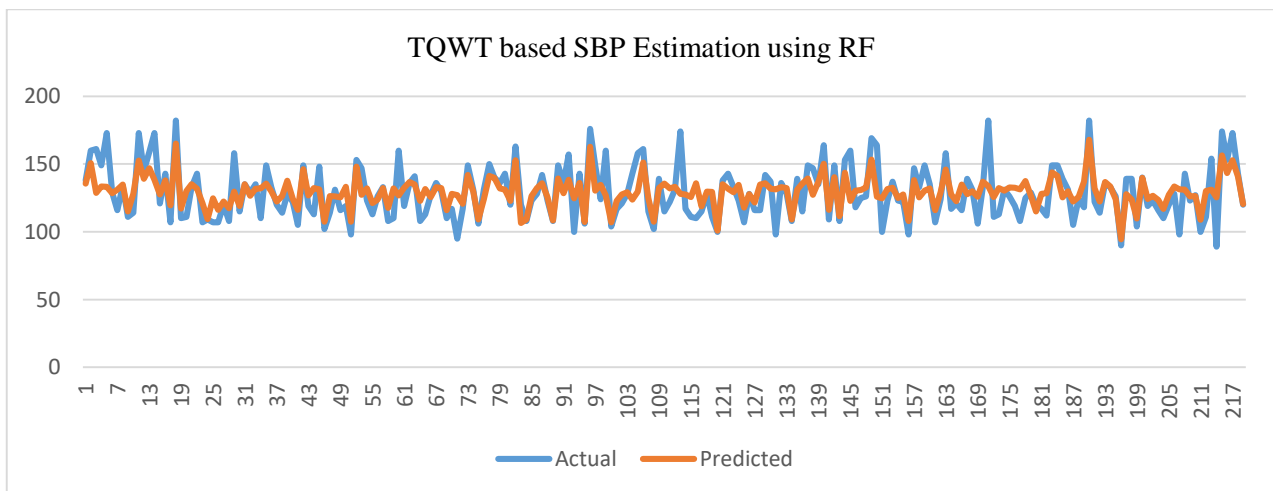


Figure 5. TQWT based SBP Estimation using RF

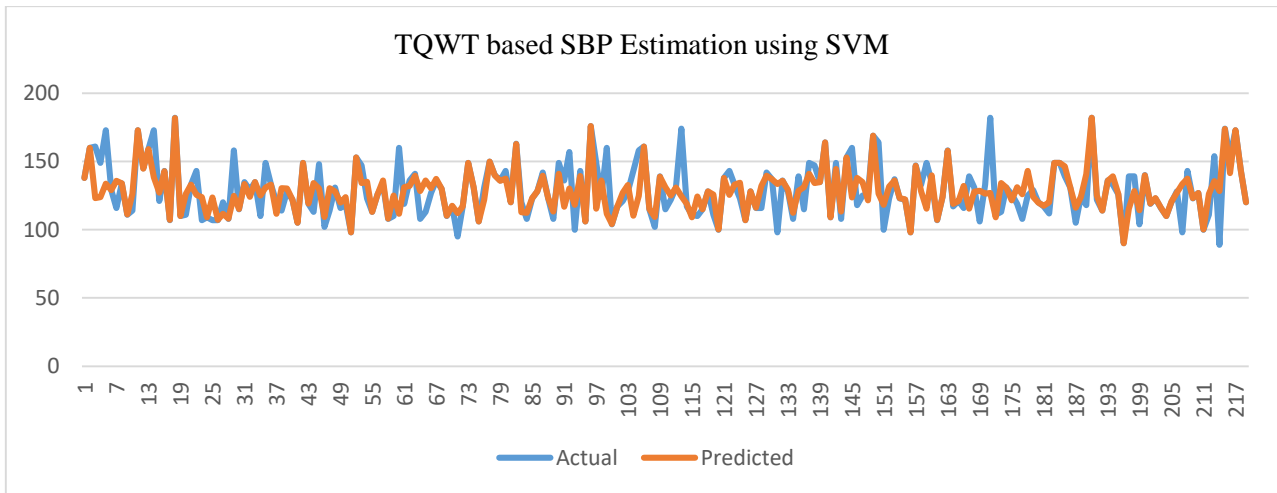


Figure 6. TQWT based SBP Estimation using SVM

Table 3. Normalized Correlations and Error Rates for TQWT based SBP Estimation

Method	CC	MAE (mmHg)	RMSE (mmHg)
ANN	0.5716	7.5628	9.2981
RF	0.8391	7.2694	8.1719
SVM	0.8107	6.7648	9.4167

HR estimations performed using ANN, RF and SVM methods can be seen in Figures 7, 8, and 9.

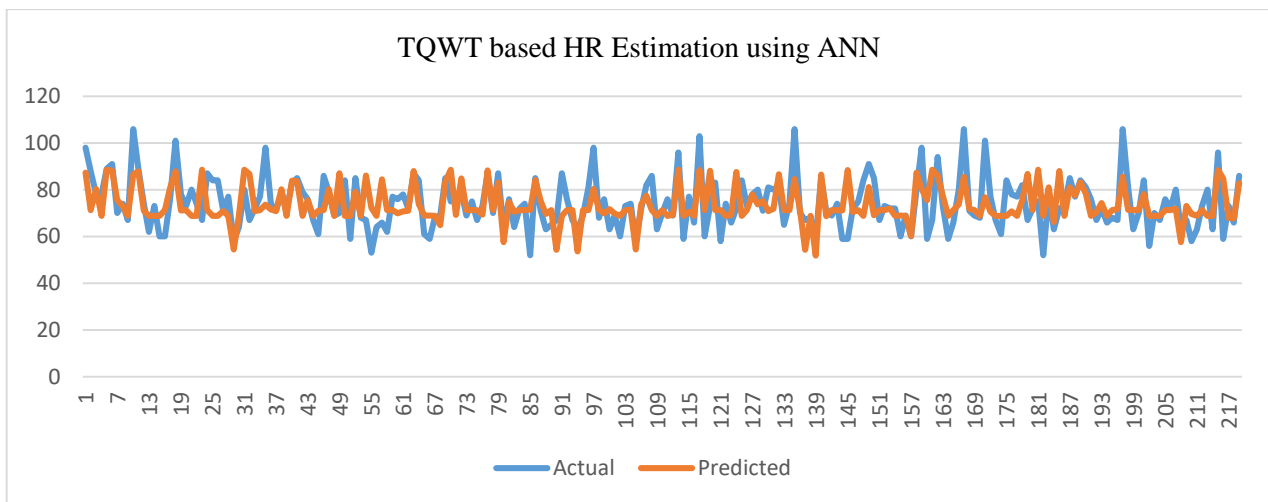


Figure 7. TQWT based HR Estimation using ANN

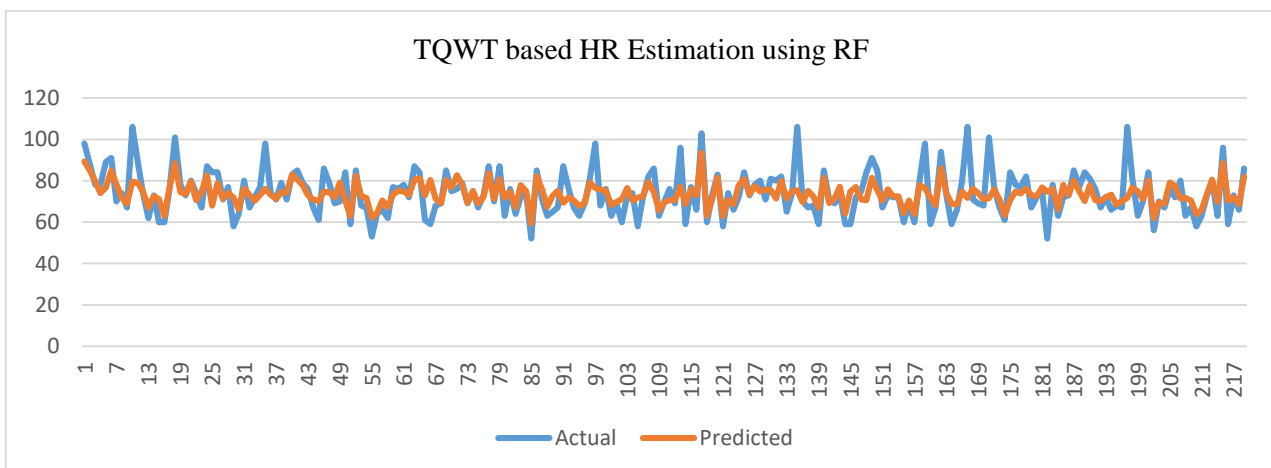


Figure 8. TQWT based HR Estimation using RF

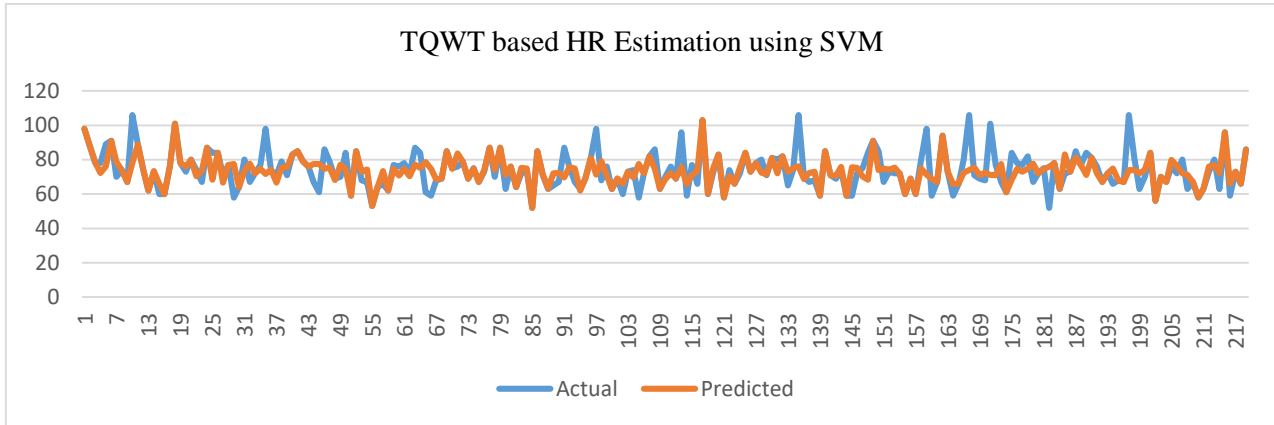


Figure 9. TQWT based HR Estimation using SVM

Table 4. Normalized Correlations and Error Rates for TQWT based HR Estimation

Method	CC	MAE	RMSE
ANN	0.6180	6.3349	8.2164
RF	0.8117	4.2946	6.8852
SVM	0.7714	3.9872	6.6285

DISCUSSIONS

Standard of the Association for the Advancement of Medical Instrumentation (AAMI) can be used to analyze the performance of BP estimations. AAMI says that for reliable BP estimation, the maximum MAE value between estimated and reference BPs must be 5 mmHg. Our results show that the MAE values are in the standard for DBP estimations with RF and SVM. However, for SBP estimations, MAE values of our results are little bit higher than the standard value. We think that the reason of this performance decrease is the high variance of SBP set. High variance makes the regression analysis more challenging.

The correlation coefficient in the estimations of DBP with the TQWT method using the RF algorithm is higher than the correlations coefficients in the estimations performed using ANN and SVM algorithms. As seen in Table 2, the error rates in the estimations performed using ANN algorithm appear to be higher than the other algorithms. Correlation coefficients show that the estimation of SBP with the TQWT method using RF algorithm is higher than the other algorithms. As seen in Table 3, no significant difference was seen between the error rates in the estimations performed with all of the machine learning algorithms.

The values of the correlation coefficients and error rates for the estimation of HR using the machine learning algorithms of ANN, RF and SVM, and the analysis method of TQWT are shown in Table 4. As it can be seen, the correlation coefficient of the estimations performed using the RF algorithm is higher than the correlation coefficients of the estimations performed using the other algorithms. The correlation coefficient of the estimations performed using the ANN algorithm is quite lower and the error rates are quite higher compared with the other algorithms. It is obvious that the ANN algorithm is not suitable for determining HR.

As it can be seen in the tables, when the CC, MAE, and RMSE values are compared one by one for each method in the BP and HR estimation study using the features extracted by the TQWT method, it is observed that the RF method yields the best results with high accuracy. When the estimations performed using the RF method, it is seen that the CC is 0.7219 for DBP, 0.8391 for SBP, and 0.8117 for HR.

CONCLUSIONS

In this paper, it was aimed to estimate BP levels and HR based on the PPG signals. The PPG signals were separated into their sub-bands using the TQWT method, and the statistical features were extracted from each sub-band and the main signal. The extracted features were subjected to regression analysis by machine learning methods, and the BP levels and HR values were estimated.

Results show that the PPG signals are very useful to monitor some important biomedical values. Easy recording and processing of PPG signals make them promising for medical applications. Monitoring the BP and HR levels using wearable devices will be possible with high accuracies in the next years.

Performance of the wavelet decomposition increases because of the flexible algorithm of TQWT. Controlling the characteristics of mother wavelet makes the method appropriate for non-stationary signals like the biomedical ones. Using of TQWT effected the results of this research positively. However, it is obvious that the proposed method needs more improvements. Some of the new and promising decomposition methods and time-frequency analysis techniques can be employed instead of TQWT for obtaining better performance.

The correlation coefficients and error rates demonstrate that the best estimation results are obtained with the RF algorithm. However, in general, estimation results are not successful enough to replace conventional measurement methods in practice. It is supposed that higher estimation results can be obtained if the features which are different from the ones used in this study and more suitable for the purpose of this study are used. For the future research, it is projected to obtain more successful estimation results by trying some new and powerful analysis methods in conjunction with the TQWT and using different time and frequency domain features of the signals. Also, using a different dataset which includes more data might improve the estimation results.

REFERENCES

- Acharya, U. R., Hagiwara, Y., Koh, J. E.W., Oh, S. L., Tan, J. H., Adam, M., and San Tan, R., (2018), Entropies for automated detection of coronary artery disease using ecg signals: A review, *Biocybernetics and Biomedical Engineering*, vol. 38, no. 2, pp. 373–384.
- Al Ghayab, H. R., Li, Y., Siuly, S., and Abdullah, S., (2019) A feature extraction technique based on tunable q-factor wavelet transform for brain signal classification, *Journal of neuroscience methods*, vol. 312, pp. 43–52,.
- Allen, J., & Murray, A.,(2003), Age-related changes in peripheral pulse shape characteristics at various body sites, *Physiological Measurement*, 24(2), 297–307.
- Allen, J.,(2007), Plethysmography and its application in clinical physiological Measurement, *Physiological Measurement*, 28(3), 1-39.
- American National Standards Institute (2023). Non-invasive sphygmomanometers - Part 2: clinical investigation of automated measurement type. ANSI/AAMI/ISO 81060–2:2013. <http://webstore.ansi.org>, Accessed September 26,.
- Bagha, S., & Shaw, L. ,(2011), A real time analysis of PPG signal for measurement of SpO2 and Pulse Rate, *International Journal of Computer Applications*, 36(11),45-50.
- Büyüköztürk, K., (1999), Turkish cardiology association national hypertension treatment and follow-up guide, <https://tkd.org.tr/kilavuz/k03.htm>, [Visited: 13/03/2021].
- Engel, T.A., Charao, A.S., Pinheiro, M.K., & Steffeneel, L.A.,(2014), Performance Improvement Of Data Mining in Weka Through GPU Acceleration, *Procedia Computer Science*, 32, 93 – 100.
- Gao, S.C., P. Wittek, L. Zhao, W.J. Jiang, (2016) Data-driven estimation of blood pressure using photoplethysmographic signals, August 2016 38th Annual International Conference of the IEEE Engineering in Medicine and Biology Society (EMBC), IEEE, pp. 766-769.
- Han, J., Pei, J., and Kamber, M., (2011) *Data Mining: Concepts and Techniques*, Elsevier, Amsterdam, Netherlands.
- Hertzman A.B., (1938), The blood supply of various skin areas as estimated by the photoelectric plethysmograph, *American Journal of Physiology*,24(2), 328– 340.
- Johnston,W.,(2006), Development of a Signal Processing Library for Extraction of SpO2, HR, HRV, and RR from Photoplethysmographic Waveforms, Thesis (Msc) Worcester Polytechnic Institute.
- Kraitl, J., Hartmut E.,(2005), Optical non-invasive methods for characterization of the human health status, 1st International Conference on Sensing Technology, 21-23 November 2005 Palmerston North, New Zealand.
- Kurylyak, Y., Lamonaca, F., and Grimaldi, D., (2013) A Neural Network-based method for continuous blood pressure estimation from a PPG signal, 2013 IEEE International Instrumentation and Measurement Technology Conference (I2MTC), , pp. 280-283.

- Liang, Y., Chen, Z., Liu, G., & Elgendi, M., (2018), A new short-recorded photoplethysmogram dataset for blood pressure monitoring in China, *Scientific Data*, 5.
- McDuff D., Gontarek S. & Picard R. W.,(2014), Remote detection of photoplethysmographic systolic and diastolic peaks using a digital camera, *IEEE Transactions on Biomedical Engineering*, 61(12), 2948-2954.
- Nafisi, V. B. & Shahabi, M, (2018), Intradialytic hypotension related episodes identification based on the most effective features of photoplethysmography signal. *Comput. Methods Programs Biomed.* 157 (4), 1–9.
- Rastegar, S., Gholamhosseini, H., Lowe, A., Mehdipour, F. and Lindén, M., (2019). Estimating Systolic Blood Pressure Using Convolutional Neural Networks, *Studies in health technology and informatics*, 261, 143-149, , PMID: 31156106.
- Schlesinger, O., Vigderhouse, N., Eytan, D. and Moshe, Y., (2020). Blood Pressure Estimation from PPG Signals Using Convolutional Neural Networks and Siamese Network, *IEEE International Conference on Acoustics, Speech, and Signal Processing (ICASSP)*, pp. 1135-1139, DOI: 10.1109/ICASSP40776.2020.9053446.
- Selesnick, I. W., (2011), Wavelet transform with tunable Q-factor, *IEEE Transactions on Signal Processing*, 59(8), 3560–3575.
- Shin H. S., Lee C., & Lee M.,(2009), Adaptive threshold method for the peak detection of photoplethysmographic waveform, *Computers in Biology and Medicine*, 39(12), 1145-1152.
- Teng, X. F. and Zhang, Y. T., (2003). Continuous and noninvasive estimation of arterial blood pressure using a photoplethysmographic approach, *Proceedings of the 25th Annual International Conference of the IEEE Engineering in Medicine and Biology Society (IEEE Cat. No. 03CH37439)*. Vol. 4. IEEE.
- Übeyli, E. D., Cvetkovic, D., & Cosic, I., (2010), Analysis of Human PPG, ECG and EEG Signals by Eigenvector Methods, *Digit. Signal Process*, 20 (3), 956–963.
- Xing, X., Sun, M., (2016). Optical blood pressure estimation with photoplethysmography and FFT-based neural networks, *Biomed. Opt. Express*, 7 (8), pp. 3007-3020.
- Yousef Q., Reaz M. B. I., Ali, M. A. M. (2012), The analysis of PPG morphology: investigating the effects of aging on arterial compliance, *Measurement Science Review*, 12(6), 266-271.